MODELING OF SPATIAL RESOLUTION EFFECTS USING DNS OF TURBULENT CHANNEL FLOW

***C. Chin*[1], *N. Hutchins*[1], *A. Ooi*[1] *and I. Marusic*[1]**

[1] ***Department of Mechanical Engineering,***
University of Melbourne,
Victoria 3010, Australia.
chincc@.unimelb.edu.au

Abstract

In this study, the effect of limited spatial resolution of hot wire anemometry (HWA) is investigated through analysis of the two dimensional energy spectra from direct numerical simulation (DNS) of turbulent channel flow at $Re_\tau \approx 934$. Various spanwise filter lengths are applied to the streamwise velocity component in order to mimic the spatial resolution of the HWA experiments. The overall effect of insufficient spatial resolution causes attenuation of the small-scale energy levels in experimental data. The attenuated energy clearly increases as the wire-length is increased and the filtered DNS results show good agreement. It is shown that small-scale energy levels are highly attenuated in the near-wall region. We introduce an empirical expression to estimate the amount of the missing energy as a function of wire length and wall-normal distance. This expression can be used to correct experimental data for the effects of attenuation due to spatial resolution to obtain a more accurate energy spectra and turbulence intensity.

1 Introduction

Despite the rapid progression of computational technology which is promoting more DNS of fully developed turbulent flow to be carried out, experiments are still leading the way for high Reynolds number turbulent flow research. Some of the more common experimental techniques include laser doppler velocimetry (LDV) (Durst et al (1976)), particle image velocimetry (PIV) (Adrian (1991)) and hot wire anemometry (HWA). Despite advances in LDV and PIV, HWA is arguably the most accurate experimental method for measurement of turbulent fluctuation offering an unsurpassed temporal and spatial resolution. However, there are at high Reynolds number, inevitable spatial resolution issues associated with HWA that have led to inconsistent data being reported in the open literature by different groups of researchers. The earliest report on spatial resolution effects on HWA experimental measurements is by Dryden et al (1937). This work was later extended by other workers like Frenkiel (1949), Wyngaard (1968), Johansson and Alfredsson (1983), Ligrani and Bradshaw (1987), Citriniti and George (1997), Chew et al (1998) and recently Hutchins et al (2009). Of these studies, the most well-known and well-cited study is by Ligrani and Bradshaw (1987) henceforth referred to as LB87. They carried out extensive investigations on the effects of the viscous scaled length l^+ of single normal hot-wire sensors and the hot-wire length to hot-wire diameter (l/d). The symbol $^+$ denotes scaling with viscous length scale, ν/U_τ, where ν is the kinematic viscosity and U_τ is the friction velocity. Readers are referred to the paper by LB87 for detailed results. The effects of spatial resolution has lead workers to formulate corrections to obtain 'true' turbulence statistics. Elsner et al (1993) proposed a theoretical correction for HWA measurements. With the advent of moderate Reynolds number DNS, Burattini et al (2007) conducted a study utilizing DNS data of isotropic turbulence to correct for under-resolved scalar measurement. Other proposed corrections using DNS for HWA are reviewed by Moin and Mahesh (1998). Correction methods proposed by Elsner et al (1993) and Burattini et al (2007) are based on the assumption of isotropic turbulence. However it has long been known (see Kline et al (1967)) that coherent motions in wall-bounded turbulent flows can be highly anisotropic, hence the assumption of using isotropic turbulence to correct hot-wire measurements would be incorrect. In order to better understand the spatial resolution effects, one would ideally require spanwise information pertaining to the width of energetic fluctuations as compared to the length of the hot-wire. It is very difficult for HWA experiments to obtain spanwise information whereas DNS data has such information readily available. We will be using DNS data of turbulent channel flow by del Álamo et al (2004) to investigate the effects of spatial resolution. The DNS has a Reynolds number $Re_\tau = U_\tau/\nu = 934$. The computational size of the domain is L_x x L_y x $L_z = 8\pi\delta$ x $3\pi\delta$ x $2\pi\delta$, where x, y & z denotes the streamwise, spanwise and wall-normal directions and δ denotes half channel height. The spatial resolutions in x and y are $\Delta x^+ \approx 7.6$ and $\Delta y^+ \approx 3.8$. Spacing in the wall-normal direction is in Chebychev polynomials. Readers are referred to the paper by del Álamo et al (2004) for more details of the simulation. The averaging process and signal attenua-

tion encountered by different wire lengths in HWA is simulated by applying a spanwise spatial averaging to the DNS data. Given the spanwise spacing of Δy^+ = 3.8 in the DNS data, filtering of the data will be restricted to multiples of Δy^+. The filter lengths considered for this study range from $l^+ \approx 11.5$ ($3\Delta y^+$), 19.1 ($5\Delta y^+$), 34.4 ($9\Delta y^+$), 57.3 ($15\Delta y^+$), 103.2 ($27\Delta y^+$) and 149.0 ($39\Delta y^+$). The process and methodology employed to filter the DNS data is similar to that of Chin et al (2009). In this paper, we will investigate the effects of spatial resolutions on turbulence statistics and formulate an empirical correction which is a function of wire length and wall normal distance to model the missing spectra energy due to attenuation of the hot-wire signals. In addition, we will also apply the equations on experimental results to verify the validity.

2 Effects of spatial attenuation

The effect of insufficient spatial resolution on the streamwise fluctuating velocity turbulence intensity ($\overline{u^2}/U_\tau^2$) is shown in figure 1. In the figure, the different profiles correspond to applying different spanwise filter lengths to the DNS data. The direction of the arrow indicates increasing filter length (l^+), it can be seen in figure 1 that increasing the filter length promotes greater attenuation of the turbulence intensity, especially in the near-wall region. As the wall-normal distance increases, the effect of spatial resolution gradually decreases and appears to diminish altogether as the centre of the channel δ is approached. The dashed-line is at wall-normal location $z^+ \approx 15$, widely accepted as the peak in turbulence intensity. It is worth noting that at $z^+ \approx 15$, the attenuation seems to be the greatest. Table 1 summarizes the amount of attenuation due to different filter lengths as compared to the 'true value' from an 'unfiltered' wire-length of $l^+ = 3.8$ at $z^+ \approx 15$. This result is as expected since a finite wire-length will have greatest effect on small-scales which are primarily dominant in the near wall region. In order to illustrate this attenuation effect on small-scales, we investigate the effects of spatial resolution on the premultiled one-dimensional energy spectra. The streamwise premultipled 1d spectra energy is calculated using the following formula,

$$\psi_{uu}(k_x, z) = k_x \langle \hat{u}(k_x, z)\hat{u}^*(k_x, z)\rangle, \qquad (1)$$

where k_x is the streamwise wave numbers, $\langle\ \rangle$ denotes spatial and temporal average, $\hat{u}$ denotes Fourier transform of u and * denotes complex conjugate. Figure 2 shows the premultipled streamwise energy spectra for $z^+ \approx 15$. Here the normalized energy spectra ψ_{uu}/U_τ^2 is plotted as a function of streamwise wavelength λ_x^+ (where $\lambda_x = 2\pi/k_x$) for the same filter lengths as figure 1. The figure clearly demonstrates that longer filter lengths, filter increasing amounts of small-scale energy from the spectra. The effect of

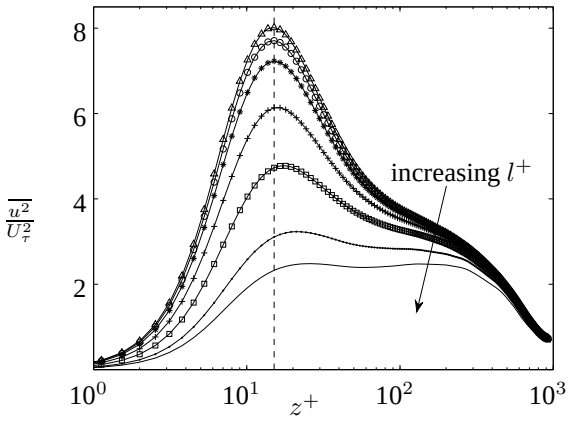

Figure 1: Turbulence intensity profiles for different filer lengths applied on DNS data, $l^+ \approx 3.8$ (Δ), 11.5 ($\circ$), 19.1 ($\star$), 34.3 ($+$), 57.3 ($\square$), 103.2 ($\bullet$) and 149.0 ($-$), arrow indicates increasing filter length (l^+), the dashed line is at $z^+ \approx 15$.

Filter length (l^+)	*Symbol*	$\overline{u^2}/U_\tau^2$ (*attenuation*, %)
3.8 (unfiltered)	Δ	-
11.5	$\circ$	3.8
19.1	$\star$	9.8
34.4	$+$	23.5
57.3	$\square$	41.0
103.2	$\bullet$	61.2
149.0	$-$	71.0

Table 1: Tabulated attenuation in percentage(%) for different wire-lengths at $z^+ \approx 15$.

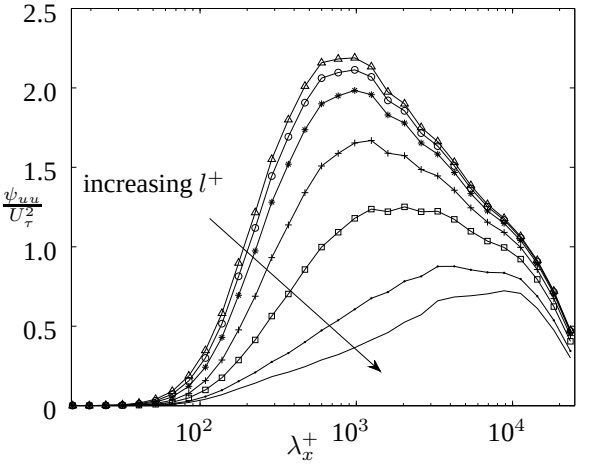

Figure 2: Premultipled streamwise one dimensional energy spectra at wall-normal location $z^+ \approx 15$ for different filter-lengths. Symbols used are as figure 1.

this attenuation of small-sclaes causes the peak of the energy spectra curves to shift towards a greater wavelength from $\lambda_x^+ \approx O(1000)$ (for $l^+ = 3.8$) to $\lambda_x^+ \approx O(10000)$ (for $l^+ = 149.0$). With DNS, we can obtain more information of the attenuated energy spectra as a function of both streamwise (λ_x^+) and spanwise (λ_y^+) wavelengths. (The 1d energy spectra in figure 2 is basically the spanwise integrand of the 2d energy spectra). Figure 3 shows the premultipled streamwise 2d energy spectra (Ψ_{uu}) for different filter lengths at wall-normal location of $z^+ \approx 15$. Figure 3 (a) shows the unfiltered ($l^+ \approx 3.8$) 2d energy spectra, figure 3 (b) and (c) shows the filtered energy at filter lengths of $l^+ \approx 34.4$ and 57.3 respectively. Figure 3 clearly shows that a longer filter length attenuates more energy. The energy attenuated seem to be fully confined to smaller wavelengths and will be discussed further in the section 3. This attenuation of the small-scales causes a shifts in the peak. This is illustrated with the '+' symbol chosen at an arbitrary location of $\lambda_x^+ = 1100$ and $\lambda_y^+ = 200$. We noticed the peak shifts towards a greater streamwise wavelength (λ_x^+) and also towards a greater spanwise wavelength (λ_y^+) as the filter length increases. This finding is consistent with the results of increasing filter lengths on the 1d energy spectra shown in figure 2, whereby a pseudo peak is observed at increasing wavelengths as l^+ is increased. In experiments, such pseudo peaks can potentially be misinterpreted, leading to misleading conclusions regarding the length of energetic fluctuations in the near wall. Together figure 1 to 3 emphasize the fact that spatial resolution of hot-wire data has significant effect on turbulence statistics and should be accounted for when interpreting results.

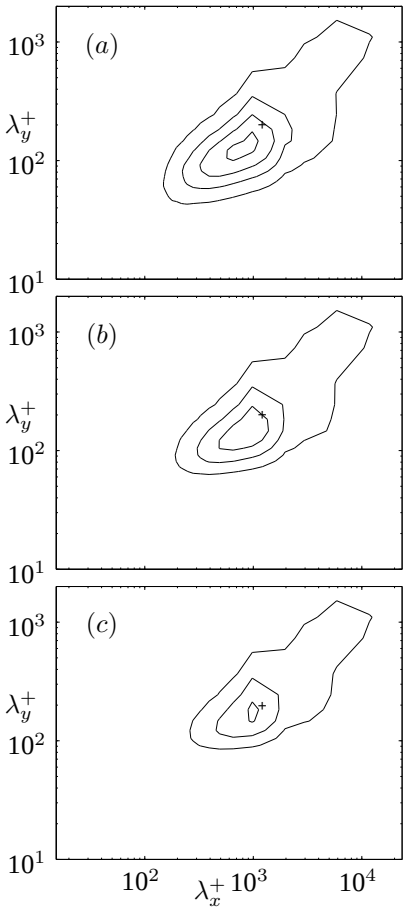

Figure 3: Premultipled streamwise two dimensional energy spectra (Ψ_{uu}/U_τ^2) at wall-normal location $z^+ = 15$ for different filter lengths of (a) $l^+ \approx 3.8$ (unfiltered), (b) $l^+ \approx 34.4$ and (c) $l^+ \approx 57.3$. The symbol '+' is at location $\lambda_x^+ = 1100$ and $\lambda_y^+ = 200$. Contour maps begin at Ψ_{uu}/U_τ^2 = 0.2 with increment of 0.25.

3 Missing Energy Model

With a clearer understanding of where the missing energy is located on a 2d spectra map, one could potentially be able to model it. Figure 4 shows the missing premulitpled 2d energy spectra using a filter length of $l^+ \approx 57.3$ at different wall-normal locations. The missing energy is calculated based on the difference between the unfiltered 2d energy spectra and the specified filtered 2d energy spectra. Figure 4 (a) shows the missing energy at $z^+ \approx 55$, (b) at $z^+ \approx 103$, (c) at $z^+ \approx 184$ and (d) at $z^+ \approx 232$. It is apparent that the missing energy is concentrated within the smaller length scales at these wall-normal locations. The missing energy is greater in the streamwise length scale (λ_x^+) than the corresponding spanwise length scale (λ_y^+). This shows that the attenuated energy is highly anisotropic and correction models (as discussed earlier) which are based on the assumption of isotropic turbulence are unlikely to work. From figure 4, the missing energy seems to resemble a Gaussian distribution which is slightly rotated in the counter-clockwise direction. It is important to note that the peak of the missing 2d energy spectra shifts slightly as the wall-normal distance increases (from figure 4 (a) to 4 (b)), but as the wall-normal distance exceeds $z^+ \approx 117$, the peak seems to settle (at location $\lambda_x^+ \approx 250$ and $\lambda_y^+ \approx 120$ as indicated by the '+' symbol). Figure 4 indicates that beyond $z^+ = 100$, the location of the peak 2d missing energy remains stationary and only the magnitudes decreases. The magnitude of the missing energy seems to stabilize for $z^+ > 184$. This is expected as large-scale motions are predominant in the outer flow region and the effect of spatial resolution is largely limited to attenuation of small-scale energy.

The model is applicable for correction up to wire-lengths of $l^+ \approx 60$. This is the maximum filter length applied so far to the DNS data to obtain the 2d missing energy spectra, from which the model is formulated. However, in theory, the model should be able to model spatial resolution effects for hot-wires of greater lengths (this will be discussed later). The primary purpose of the correction model is to aid experimentalists to obtain a better approximation of the 'true' turbulent energy in situations where inade-

quate spatial resolution is an unavoidable issue (i.e. at high Reynolds numbers). The intention here is not to encourage usage of large hot-wire lengths in experiments. An empirical expression to model the missing 2d energy as a function of streamwise and spanwise wavelengths, wire-length and wall-normal distance is derived in the form

$$f(\lambda_x^+, \lambda_y^+, l^+, z^+) = A \exp\left(-\left[\frac{(\alpha-\alpha_0)^2}{\sigma_\alpha} + \frac{(\beta-\beta_0)^2}{\sigma_\beta}\right]\right). \quad (2)$$

The term A is a function of wall-normal and filter length ($A = f(z^+, l^+)$) and the exponential term essentially represents a skewed 2d gaussian bump. More details of the constants will be in a forthcoming paper. Once the 2d missing energy is obtained, one could easily integrate across the spanwise wavelength to obtain the missing 1d streamwise energy spectra. The model is formulated using DNS data at quite low Reynolds number. However the true practicality of this model would lie in the application to higher Reynolds number flows. In an attempt to demonstrate this, the model is used to correct boundary layer data of Hutchins et al (2009) at $Re_\tau \approx 7400$ and 14000 (which is almost 8 to 15 times greater than Reynolds number of the DNS). Figures 5 demonstrates how the missing model can be used to correct 1d spectra at different wall-normal locations and with different wire-lengths. In the first column of figure 5, the Reynolds number is $Re_\tau \approx 7400$ at wall-normal locations of $z^+ \approx 25$. The second column shows results for $Re_\tau \approx 14000$ at $z^+ \approx 70$. Figure 5 (a) shows the experimental results of 1d premultipled energy spectra (ψ_{uu}/U_τ^2) for three different hot-wire lengths of $l^+ \approx 11$, 22 and 79 (solid line, dashed line and dot-dash line respectively) at $Re_\tau \approx 7400$. Figure 5 (b) shows similar data at $l^+ \approx 22$, 79 and 153 (solid line, dashed line and dot-dash line respectively) for $Re_\tau \approx 14000$. Together these plots clearly show the attenuation of the small-scales as the hot-wire length increases. The attenuated energy can be modeled using the integrand of equation 2. Figure 5 (c) and (d) show the modeled missing 1d energy spectra according to the three different wire lengths used. Figure 5 (e) and (f) are the corrected spectra which essentially are obtained by adding the measured attenuated energy spectra curve (figure 5 a and b) with the modeled missing energy (figure 5 c and d). All corrected spectra seem to collapse reasonably well. Having validated the ability of the model to correct the 1d energy spectra, we next extend the use of the missing energy model to correct the turbulence intensities (the attenuated turbulence intensities are the integrand of the missing 1d energy spectra or the direct double integrand of equation 2). Again, we will use the same experimental boundary layer data to validate the model for turbulence intensity corrections.

Figure 6 (a) and (b) shows the streamwise turbulence intensities for $Re_\tau \approx 7400$ and 14000 respectively, the hot-wire lengths used are the same in figure 5. Figure 6 (c) and (d) display the corrected turbulence intensities for $Re_\tau \approx 7400$ and 14000 respectively. The corrected results seem to agree relatively well to the shortest hot-wire length profile ($l^+ \approx 11$ for $Re_\tau \approx 7400$ and $l^+ \approx 22$ for $Re_\tau \approx 14000$). These findings provide evidence that the missing energy model formulated from low Reynolds number DNS can be accurately used to correct actual experimental results

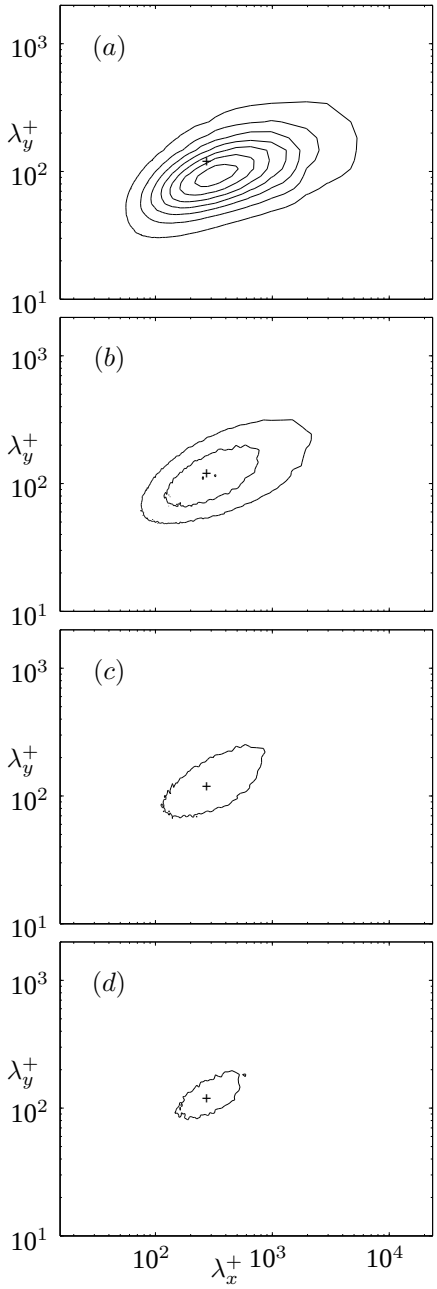

Figure 4: Premultipled streamwise two dimensional missing energy spectra (Ψ_{uu}/U_τ^2) at wall-normal location; (a) $z^+ \approx 55$, (b) $z^+ \approx 103$, (c) $z^+ \approx 184$ and (d) $z^+ \approx 232$ for filter length of $l^+ \approx 57.3$. The symbol '+' is at location $\lambda_x^+ = 250$ and $\lambda_y^+ = 120$. Contour maps begin at 0.02 with increment of 0.02.

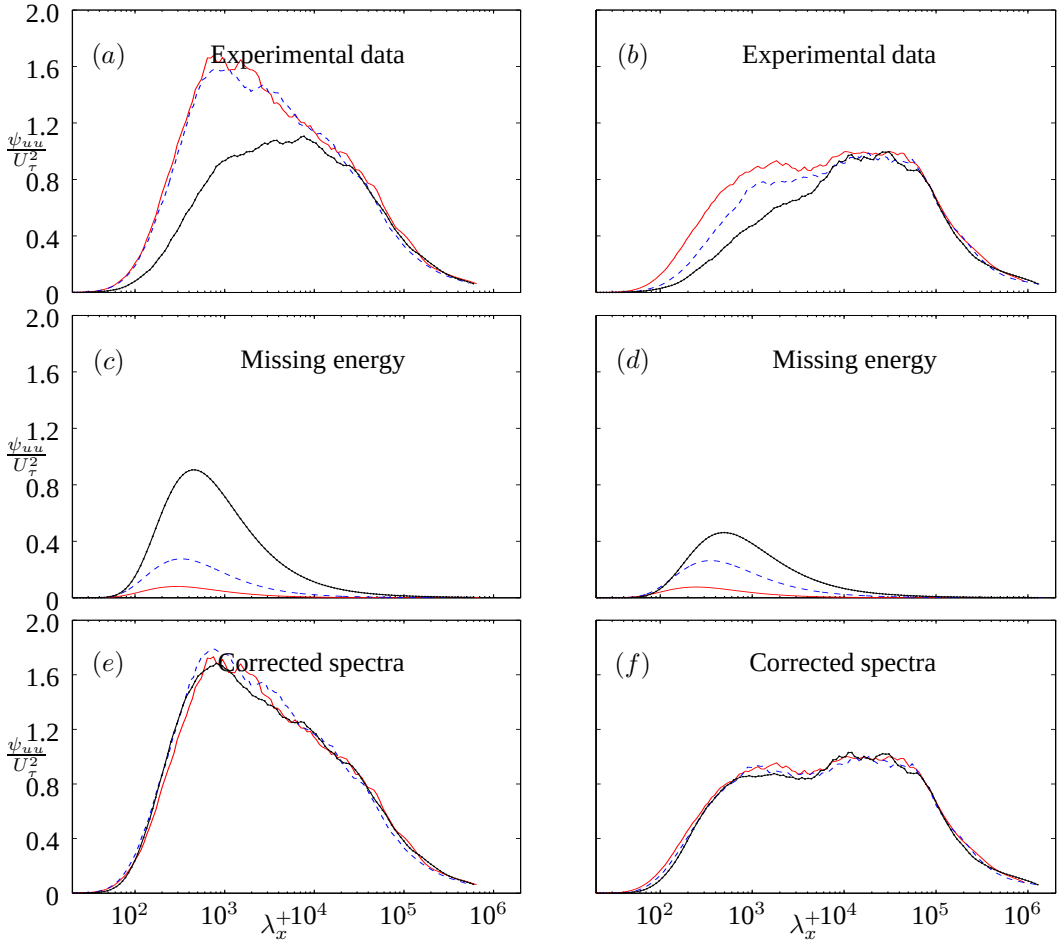

Figure 5: Comparison of corrected energy spectra. (a) actual experimental results, (c) missing energy from equation 2 and (e) the corrected energy spectra, at wall-normal location $z^+ \approx 25$ for boundary layer experimental data at $Re_\tau \approx 7390$ for three different hot-wire lengths of $l^+ \approx 11$ (red solid line $-$), $l^+ \approx 22$ (blue dashed-line $--$) and $l^+ \approx 79$ (black dot-dashed line $- \bullet -$). (b) actual experimental results, (d) missing energy from equation 2 and (f) the corrected energy spectra at $z^+ \approx 70$ for $Re_\tau \approx 14000$ using hot-wire lengths of $l^+ \approx 22$ (red solid line $-$), $l^+ \approx 79$ (blue dashed-line $--$) and $l^+ \approx 153$ (black dot-dashed line $- \bullet -$).

at far higher Reynolds numbers.

4 Conclusions

This study investigated the effects of insufficient spatial resolution in HWA by applying a filtering method to DNS channel flow data. The results show that attenuation of the turbulence intensity increases as the filter length increases. This attenuation is more severe in the near-wall region, mainly because small-scales structures are more dominant in this region and as such this region is more susceptible to attenuation due to insufficient spatial resolution. This attenuation of small-scales in the near-wall region is confirmed by the 1d and 2d filtered energy spectra. More importantly, the energy spectra suggest that the large scales are mostly unaffected by spatial resolution, which suggest that a correction modeling viscous-scaled attenuation could work at higher Reynolds numbers. An empirical equation has been formulated to model the missing 2d energy spectra for different filter length and different wall-normal distances. The 2d missing energy model can be integrated across the spanwise length-scale to correct experimental 1d energy spectra results. A double integrand of the missing energy model can be utilized to correct turbulence intensity profiles. Validation of the missing energy model is performed using experimental boundary layer data and shown to be suitable. This is in-spite of the fact that the experiment is carried out at a much higher Reynolds number. The ability of the model to work at higher Reynolds number reinforces the finding of Hutchins et al (2009) who showed that viscous-scaled small-scale energy is invariant with Reynolds number in the near-wall and logarithm regions. It is this viscous-scaled small-scale attenuation that is modeled by the correction scheme. Only the large-scales exhibit Reynolds number variation, and these are shown to be largely immune to spatial resolution effects.

Acknowledgments

The authors are gratefully to Professor R D Moser

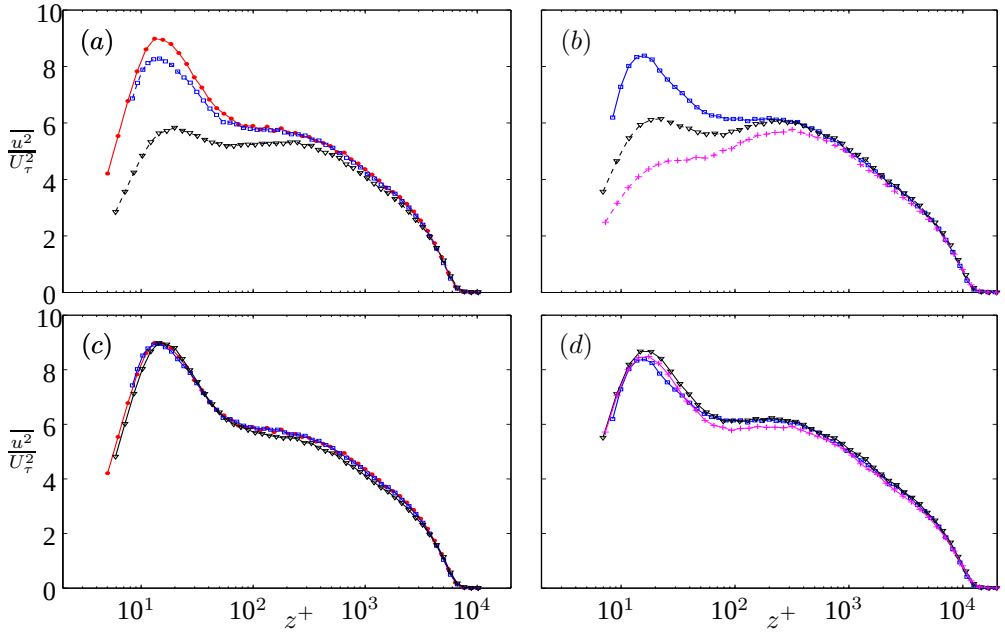

Figure 6: Comparison of turbulence intensity profiles. Actual experimental results (a) for filter lengths $l^+ \approx 11$ (–•–), 22 (- □ -) & 79 (- ▽ -) for $Re_\tau \approx 7300$ and (b) $l^+ \approx 22$ (—□—), 79 (- ▽ -) & 153 (- + -) for $Re_\tau \approx 14000$. (c) the corrected turbulence intensity for $Re_\tau \approx 7400$ to $l^+ \approx 11$ for $l^+ \approx 22$ (–□–) & 79 (—▽—). (d) the corrected turbulence intensity for $Re_\tau \approx 14000$ to $l^+ \approx 22$ for $l^+ \approx 79$ (—▽–) & 153 (–+–).

for making the DNS data available, and also the Australian Partnership for Advanced Computing (APAC) and the Victorian Partnership for Advanced Computing (VPAC) for the computational time. This work is financially supported by the Australian Research Council (ARC).

References

Adrian, R. J. (1991), Particle imaging techniques for experimental fluid mechanics, *Annu. Rev. Fluid Mech.*, Vol. 23, pp. 261 - 304.

Burattini, P., Kinet, M., Carati, D. and Knaepen, B. (2007), Corrections for underresolved scalar measurements in turbulent flows using a DNS database, *Exp. Fluids*,Vol. 43,pp. 31 - 37.

Chew, Y. T., Khoo, B. C. and Li, G. L. (1998), An investigation of wall effects on hot-wire measurements using a bent sublayer probe, *Meas. Sci. Technol.*, Vol. 9,pp 67 - 85

Chin, C. C., Hutchins, N., Ooi, A. S. H., and Marusic, I. (2009), Use of direct numerical simulation (DNS) data to investigate spatial resolution issues in measurements of wall-bounded turbulence, *Meas. Sci. Technol.*, Vol. 20, 115401.

Citriniti, J. H. and George, W. K. (1997), The reduction of spatial aliasing by long hot-wire anemometer probes, *Exp. Fluids*,Vol. 23,pp. 217 - 224.

del Álamo J. C., Jiménez J., Zandonade P. and Moser R. D. (2004), Scaling of the energy spectra of turbulent channels, *J. Fluid Mech.*, Vol. 500, pp. 135 - 144.

Dryden, H. L., Shubauer, G. B., Moch, W. C. and Skramstad, H. K. (1937), Measurements of intensity and scale of wind tunnel turbulence and their relation of the critical Reynolds number of spheres, *NACA Technical Report*, Vol. 581, pp. 109 - 140.

Durst, F., Melling, A. and Whitelaw J. H. (1976), Principles and Practice of Laser Doppler Anemometry, (New York: Academic).

Elsner, J. W., Domagala, P. and Elsner, W. (1993), Effect of finite spatial resolution of hot-wire anemometry on measurements of turbulence energy dissipation , *Meas. Sci. Technol.*, Vol. 4, 517 - 523.

Frenkiel, F. N. (1949), The influence of the length of a hot wire on the measurements of turbulence, *Phys. Rev.*, Vol. 75, pp. 1263 - 1264.

Hutchins, N., Nickels, T. B., Marusic, I. and Chong, M. S. (2009), Hot-wire spatial resolution issues in wall-bounded turbulence, *J. Fluid Mech.*, Vol. 635,pp. 103 - 136.

Hutchins, N. and Marusic, I. (2007), Evidence of very long meandering features in the logarithmic region of turbulent boundary layers, *J. Fluid Mech.*, Vol. 579, pp.1 - 28.

Johansson, A. V. and Alfredsson, P. H. (1983), Effects of imperfect spatial resolution on measurements of wall-bounded turbulent shear flows, *J. Fluid Mech.*, Vol. 137,pp. 409 - 421.

Kline, S. J., Reynolds, W. C., Schraub, F. A. and Runstandler, P. W. (1967), The structure of turbulent boundary layer, *J. Fluid Mech.*, Vol. 30,pp. 741 - 773.

Ligrani P. M. and Bradshaw P. (1987), Spatial resolution and measurement of turbulence in the viscous sublayer using subminiature hot-wire probes, *Exp. Fluids*, Vol. 5, pp. 407 - 417.

Moin, P. and Mahesh, K. (1998), Direct numerical simulation: a tool in turbulence research,*Annu. Rev. Fluid Mech.*,Vol. 30, pp. 539 - 578.

Monty, J. P., Stewart, J. A., Williams, R. C. and Chong, M. S. (2007), Large-scale features in turbulent pipe and channel flows, *J. Fluid Mech.*, Vol. 589, pp, 147 - 156.

Wyngaard, J. C. (1968) Measurement of small-scale turbulence structure with hot wires, *J. Phys. E: Sci. Instrum.*,Vol. 1,pp. 1105 - 1108.